

Optimal Design of an Electric Vehicle Frame Based on Response Surface Analysis

Jian Zhang*, Wei Ran, Xuemei Qi

School of Institute of Intelligent Manufacturing, Panzhihua University, Panzhihua, SiChuan, China

**Corresponding Author.*

Abstract

Aiming at the lightweight optimization problem of electric commercial vehicle frames, a multi-objective optimization method combining response surface method with MOGA (Multi-Objective Genetic Algorithm) optimization algorithm is proposed. Based on ANSYS Workbench, the finite element model was established, and the comprehensive influence of the size of longitudinal beam and cross beam on the lightweight of frame was explored. Through Central Composite Design, the second-order response surface models which affect the weight, the maximum deformation, the maximum equivalent stress, the seventh frequency and the eighth frequency was established. Took the size of frame longitudinal and cross beam as design variables, multi-objective optimization function for mass, stress, deformation and natural frequency was established. The MOGA optimization algorithm was used to optimize the model and obtained an optimized solution. The verification results show that the weight of the original frame is reduced from 314.42kg to 284.76kg, a decrease of 9.43%. The maximum stress of the frame is reduced from 189.86Mpa to 179.8Mpa, and the structure is more reasonable. The vibration frequency of the frame can stagger the vibration frequency of the road excitation and human organs when the vehicle is running normally, and the probability of resonance electromotion with the motor is small. The lightweight optimization design method has good feasibility.

Keywords: *Electric vehicle, frame, response surface, optimization, MOGA optimization algorithm*

I. Introduction

With the aggravation of environmental problems, the production and use of electric vehicles have been promoted. The research shows that if the mass of electric vehicle is reduced by 500kg, the driving range will be increased by 0.15%, and the energy consumption per 100km will be reduced by 2.75%, which can effectively increase the driving range and reduce the energy consumption per 100km [1-2]. The frame is the main load-bearing part of the car, and reducing the weight of the frame is an important means to achieve lightweight [3-4].

At present, the lightweight optimization of the frame mostly focuses on the maximum response value under a certain working condition as the constraint object, or takes the parameters of individual parts as the design variables, without fully considering the influence of different working conditions, which affects the optimization effect to a certain extent [5]. In essence, response surface method is an approximate simulation method, in which the equation is fitted by data, and the polynomial function is established to fit the design object. The equation can be expressed on the coordinate diagram, and the influence of different conditions on the response value can be predicted by the equation. Among modern optimization algorithms, genetic algorithm has unique advantages in solving nonlinear and multi peak optimization problems.

Taking the frame of a light electric commercial vehicle as the research object, the static characteristics of the frame are analyzed by ANSYS software to determine whether the strength and stiffness of the frame meet the service conditions. Taking the minimum of frame mass, maximum deformation, maximum stress and the maximum of the seventh and eighth natural frequencies as the optimization objectives, the response surface method is combined with the MOGA (Multi-Objective Genetic Algorithm) optimization algorithm to realize the multi-objective optimization of the design parameters of the main stressed parts of the frame, and obtain the optimal solution of the optimization

objectives such as frame mass and dynamic and static characteristics.

II. Frame Structure and Parameter Design

2.1 Design of frame matching parameters

According to the structure of the frame, the frame is divided into side beam type, middle beam type and comprehensive frame. Considering that the structure of the target frame is simple, the process requirements are low, and the bearing capacity and torsional stiffness are strong, so the main body adopts the front and rear equal width, equal section side beam structure.

There are box, I-shape, groove and so on in the frame longitudinal beam section, in order to ensure the function of the frame and improve the stability of the whole vehicle, a rectangle with a length of 110mm and a thickness of 8mm is selected as the longitudinal beam section, and the effective length of the longitudinal beam is 4200mm. The crossbeam of the frame is generally grooved, tubular, square, etc, in order to increase the bending capacity of the frame, the cross section of the crossbeam is $\varnothing 80\text{mm}$ cylindrical, and the width of the frame is 950mm.

2.2 Frame material selection

Compared with traditional steel, TC4 has obvious performance advantages [6]. The performance parameters of TC4 are shown in Table 1 [7].

Table 1 Mechanical properties of TC4

Material science	Yield limit (MPa)	Elastic modulus(N/mm ²)	Density(kg/m ³)	Poisson's ratio
TC4	836	1.09×10^5	4450	0.3

2.3 Load size and load form

The automobile will be subjected to various loads. When establishing the finite element model of the frame structure, in order to make the load easy to be applied on the elements and nodes, the load must be properly treated. The frame load is shown in Table 2 [7].

Table 2 Load on frame

Load name	Load value/N	Loading position	Direction
Member	1300	Third crossbeam	-Z
Drive motor	730	Second crossbeam	-Z
Power battery	1200	Third crossbeam	-Z
Full load of goods	4000	Evenly distributed on the (7-9) beams	-Z
Body load	4000	Evenly distributed on two longitudinal beams	-Z

(The direction Z is vertical upward)

III. Analysis of Static and Dynamic Characteristics of Frame

3.1 Finite element analysis model and simulation conditions

In the calculation process, in order to reduce the workload, the corresponding accessories of the geometric model of the frame are simplified, and the simplified model of the frame is established. The finite element model of the frame is shown in Figure 1.

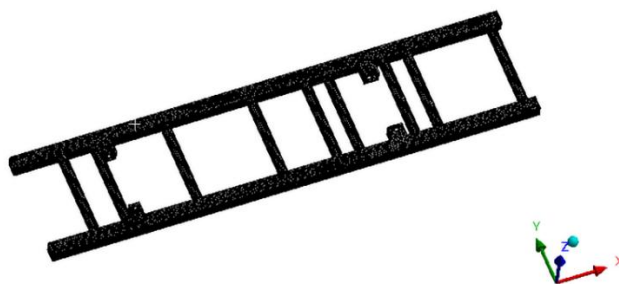


Fig1: Finite element model of frame

When the car is in motion, it will produce torque and additional load to the frame due to the turning, emergency braking, braking and road conditions. Among them, the bending condition and torsion condition have the greatest influence. Static analysis of the frame is to solve the stress and deformation parameters of the frame under different working conditions. The dynamic load coefficient is related to the stiffness of the front and rear wheel suspension system, road constant, empirical constant and driving speed [8]. In the static analysis of the frame, the dynamic load factor should be introduced. The bending condition and torsion condition are analyzed. The dynamic load coefficients of bending condition and torsion condition are 2.0 and 1.1 respectively. According to the principle of static equivalence, the equivalent load of each component is applied to the corresponding position. The boundary conditions in the frame bending condition are to constrain the degrees of freedom of the right front wheel in the X and Z directions, constrain the degrees of freedom in the X, Y, and Z directions of the left front wheel, constrain the degrees of freedom in the X direction of the right rear wheel, and constrain the X, Y directions of the left rear wheel Degrees of freedom. Under the frame torsion condition, the boundary conditions are to constrain the freedom of the right front wheel in the X, Y, and Z directions, constrain the freedom of the left front wheel in the X and Z directions, constrain the freedom of the right rear wheel in the X and Y directions, and release all the freedom of the left rear wheel Spend.

3.2 Static characteristic analysis of frame

Full load bending condition is the most commonly used basic working condition of commercial vehicle, that is, when the vehicle is full load, the wheels are on the ground, and the vehicle runs straight on a good horizontal road, the stress distribution and deformation of the frame are analyzed [9-10].

The calculation formula of bending stiffness is as follows:

$$k_b = \frac{F_l}{b_{max}} \quad (1)$$

Where, k_b -- bending stiffness, b_{max} -- average value of maximum displacement of left and right longitudinal beams in X direction, F_l -- force of left and right longitudinal beams in X direction.

Torsion condition is to simulate the ability of the frame to resist torsion and deformation when the right rear wheel is suspended under the condition of full load [11]. The calculation formula of torsional stiffness is as follows:

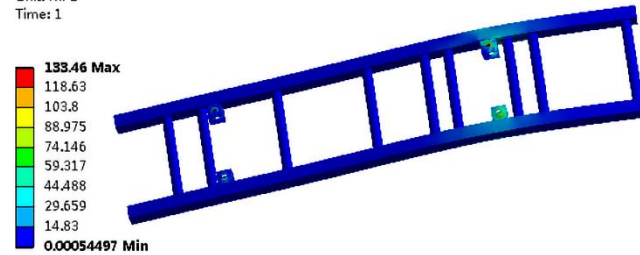
$$k_i = \frac{F_2 d_2}{\arctan(d_1 / d_2)} \quad (2)$$

Where k_i -- torsional stiffness, F_2 -- load on the frame, d_1 -- X-direction relative displacement of left and right longitudinal beams under torque, d_2 -- distance between the centers of left and right longitudinal beams.

As mentioned before, the frame boundary conditions are constrained, and the equivalent load is multiplied by the

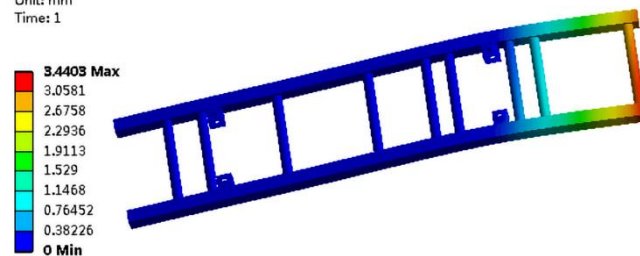
dynamic load coefficient to load. After submitting the calculation, the stress and deformation diagrams under bending and torsion conditions are obtained, as shown in Figure 2.

A: Static Structural
Equivalent Stress
Type: Equivalent (von-Mises) Stress
Unit: MPa
Time: 1



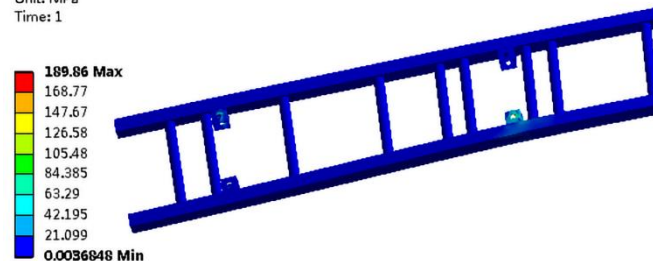
(a) Stress and deformation diagram under bending condition

A: Static Structural
Total Deformation
Type: Total Deformation
Unit: mm
Time: 1



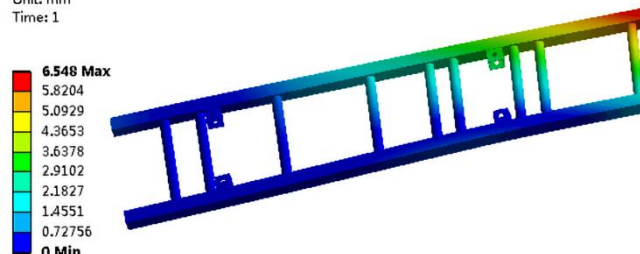
(b) Displacement and deformation diagram under bending condition

A: Static Structural
Equivalent Stress
Type: Equivalent (von-Mises) Stress
Unit: MPa
Time: 1



(c) Stress deformation diagram under torsion condition

A: Static Structural
Total Deformation
Type: Total Deformation
Unit: mm
Time: 1



(d) Displacement and deformation diagram under torsion condition

Fig2: Stress and deformation diagram under bending and torsion conditions

The results are as follows,

(1) It can be seen from Fig. 2 (b) that the deformation of the frame under bending condition mainly occurs at the rear end, and the maximum displacement is 3.44mm. The main reason is that this is the location of the goods, and the load is large. According to equation (1), the bending stiffness $k_b = 6528.5\text{N/mm}$. The maximum deformation of frame under torsion condition in Figure 2 (d) is 6.54mm. The torsional stiffness $k_t = 29732.32\text{N.m.rad}^{-1}$ is calculated by formula (2). Through the stiffness analysis, the frame has enough bending stiffness and torsional stiffness to resist the bending deformation and torsional deformation caused by external excitation.

(2) According to figure 2, the maximum stress of the frame appears at the position of the rear wheel, the maximum stress under bending condition is 133.4MPa, and the maximum stress under torsion condition is 189.86MPa, which is far less than the yield stress of TC4, indicating that the frame has further optimization space.

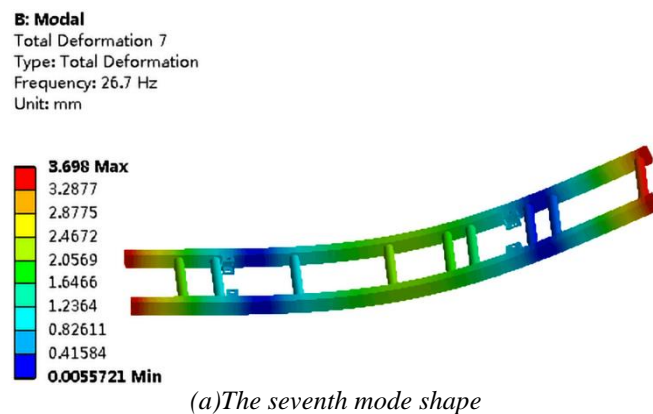
3.3 Modal analysis of frame

Modal analysis is a technology to determine the vibration characteristics of structure. Through modal analysis, the natural frequency, mode shape and mode participation coefficient of structure can be determined. In the free modal analysis of the frame, the lower mode shape has a great influence on the dynamic characteristics of the frame, so the first 12 modes of the frame are extracted. Because the frequency of the first 6 modes is lower than 1Hz, the first 6-order mode can be regarded as rigid body mode. The latter 6 non rigid mode can be analyzed. The natural frequency of the first 12 orders of the frame is shown in Table 3.

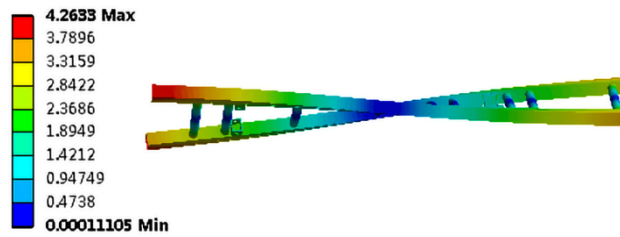
Table 3 First 12 natural frequencies of frame

Serial number	Frequency/HZ	Mode shapes
1-6	0	Rigid mode
7	26.7	Longitudinal bending
8	42.08	Bending torsion
9	72.42	Longitudinal bending
10	72.48	Lateral bending
11	87.19	Bending torsion
12	114.53	Lateral bending

The mode of vibration is shown in Figure 3.

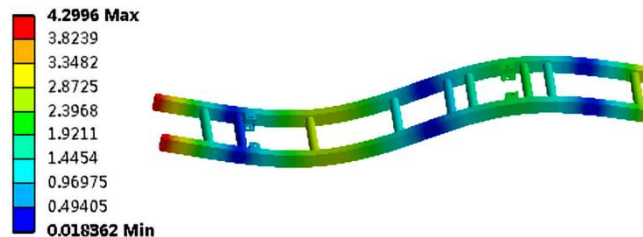


B: Modal
Total Deformation 8
Type: Total Deformation
Frequency: 42.089 Hz
Unit: mm



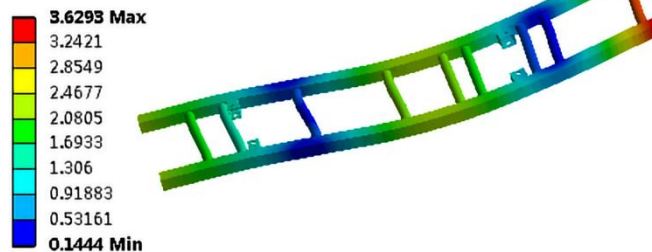
(b) The eighth mode shape

B: Modal
Total Deformation 9
Type: Total Deformation
Frequency: 72.422 Hz
Unit: mm



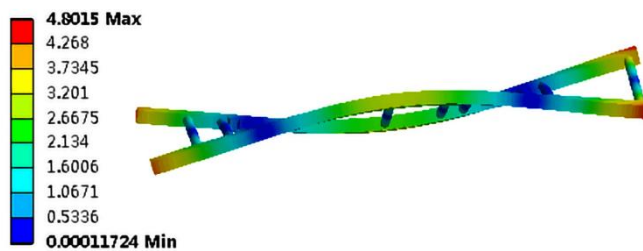
(c) Mode mode of the ninth order

B: Modal
Total Deformation 10
Type: Total Deformation
Frequency: 72.487 Hz
Unit: mm

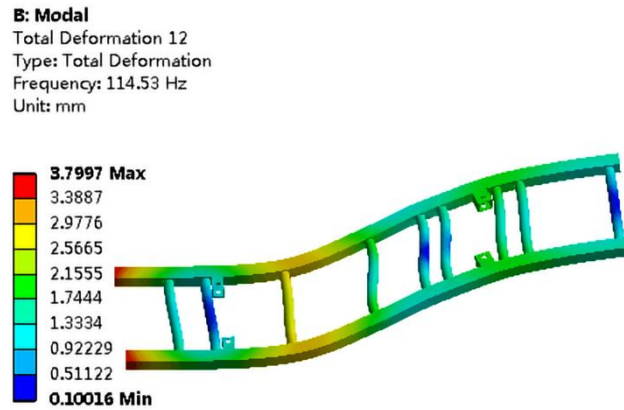


(d) The tenth mode shape

B: Modal
Total Deformation 11
Type: Total Deformation
Frequency: 87.197 Hz
Unit: mm



(e) The eleventh mode shape



(f) The twelfth mode shape
Fig 3: Modal shape diagram

The results are as follows: (1) Because the urban road is flat, the road excitation is generally lower than 20Hz when the vehicle is running normally; The vibration frequency of human organs is lower than 17Hz. It can be seen from Table 3 that the low-order modal frequency of the frame can effectively stagger the vibration frequency of human organs and the excitation frequency of the road, so as to avoid resonance. (2) The excitation frequency of automobile driving motor is 20 ~ 2000Hz [12], and the coincidence rate of frame frequency and motor excitation frequency is less than 5%. The resonance probability of automobile in the process of driving is small, so the dynamic characteristics of the frame can be improved by changing the main size of the frame.

IV. Frame Response Surface Analysis

4.1 Determination of design variables

The frame is mainly composed of longitudinal beam and cross beam. The longitudinal beam plays a bearing role and the cross beam plays a supporting role. If all the dimensions of the whole frame are taken as the design parameters, the amount of calculation will be too large. Therefore, the main bearing part of the frame is taken as the design variable, and the design part is shown in Figure 4.

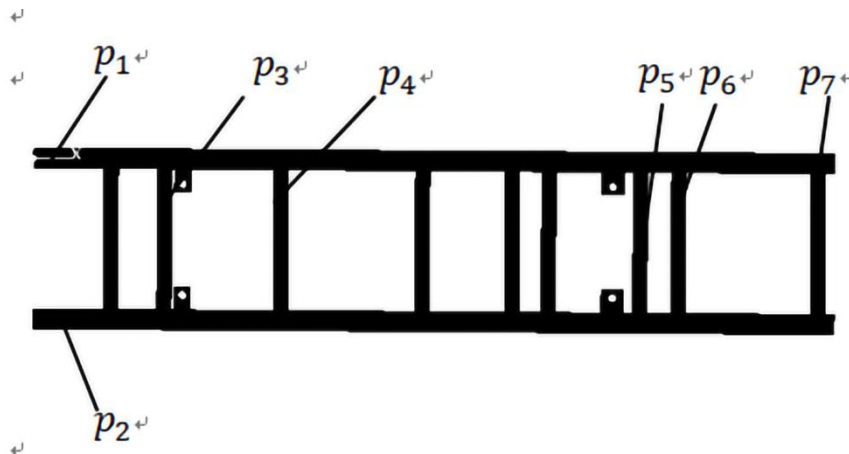


Fig 4: Design position

Based on the original structure of the frame which should not be changed, the variation range of design variables is given. The design variables are shown in Table 4.

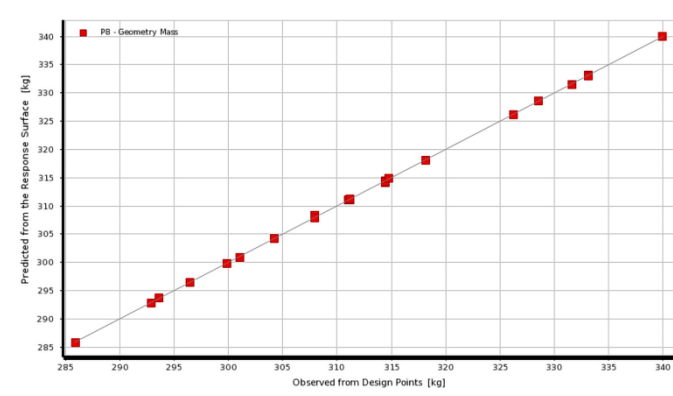
Table 4 Design variable

Design variable	Initial value/mm	Range of variation/mm
p_1	110	100~120
p_2	110	100~120
p_3	40	36~44
p_4	40	36~44
p_5	40	36~44
p_6	40	36~44
p_7	40	36~44

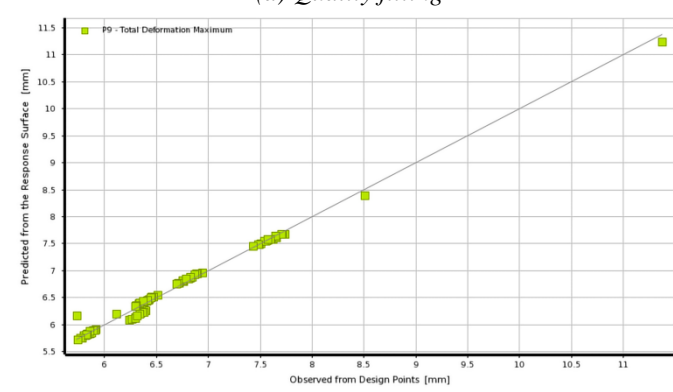
4.2 Doe experimental design

Because there are seven design variables, the Central Composite Design method is selected in the experimental design of the frame design variables. The total number of DOE tests is 97. The weight p_8 , the maximum deformation p_9 , the maximum equivalent stress p_{10} , the seventh frequency p_{11} and the eighth frequency p_{12} of the frame are taken as the output variables.

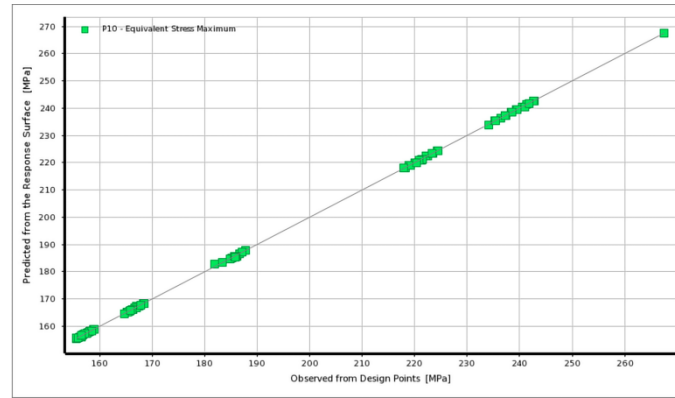
After the completion of the experimental design, the accuracy test is carried out to check the fitting effect between the predicted response value and the actual response value of each target. The fitting effect of each model is shown in Figure 5.



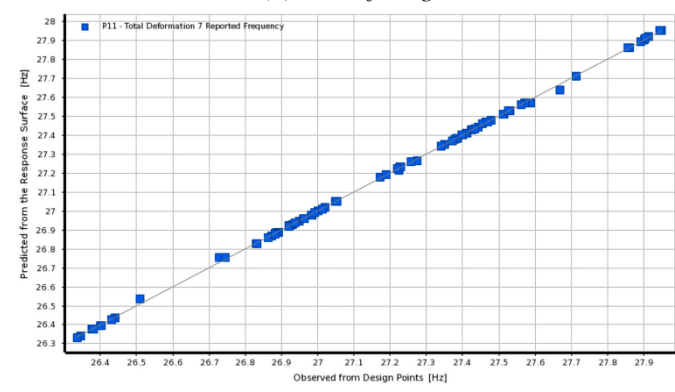
(a) Quality fitting



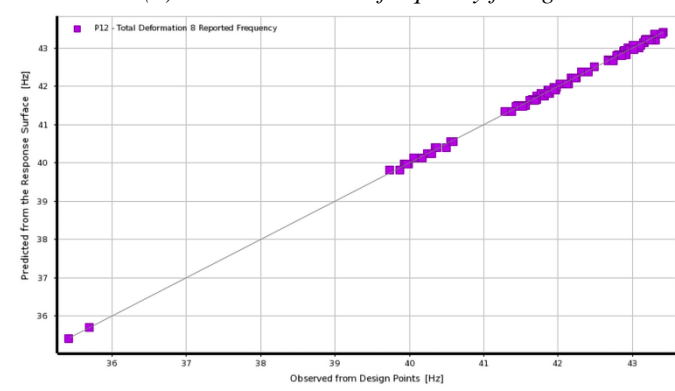
(b) Deformation fitting



(c) Stress fitting



(d) The seventh order frequency fitting

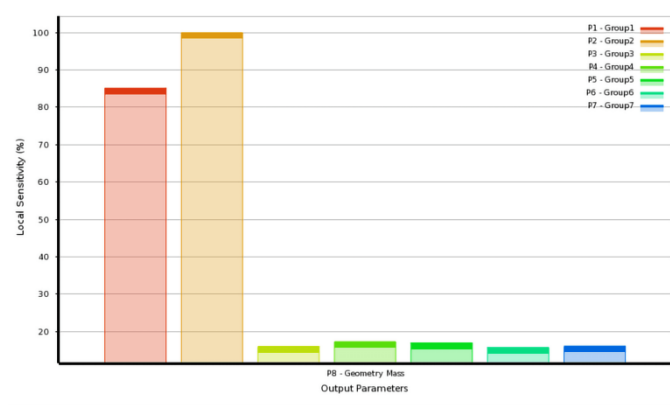


(e) The eighth order frequency fitting

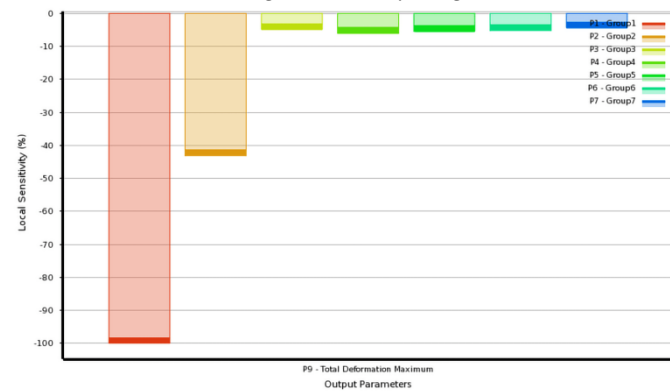
Fig 5: Fitting effect of each model

When testing the fitting accuracy of the model, the fitting effect is generally evaluated by the R^2 value of the determination coefficient [13]. It can be seen from Figure 5 that the stress fitting effect is relatively dispersed compared with the other four parameters. The main reason is that the location of the maximum stress of the frame at different design points is uncertain, and the determination coefficient R^2 is above 0.99, so the error is very small. The determination coefficients R^2 of other models are all above 0.99, the fitting effect of each model is good, and the accuracy test is qualified.

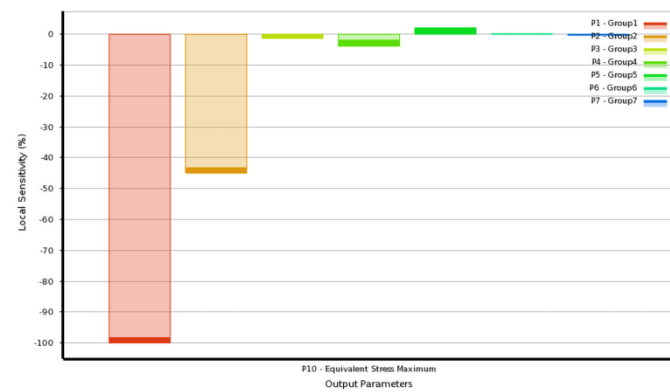
In order to determine whether the selection of design variables is reasonable, the influence of design variables on output parameters can be obtained through sensitivity analysis, so as to determine whether it is necessary to ignore some variables whose sensitivity effect is not ideal, so as to improve the calculation time. The results of sensitivity analysis are shown in Figure 6.



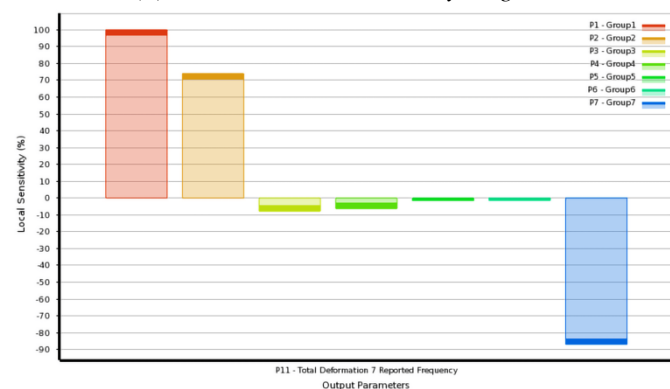
(a) Weight sensitivity diagram



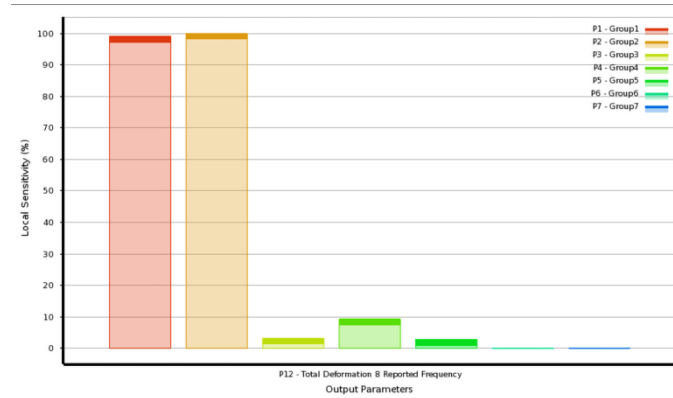
(b) Maximum deformation sensitivity diagram



(c) Maximum stress sensitivity diagram



(d) Seventh order natural frequency sensitivity diagram



(e) Sensitivity diagram of the eighth natural frequency
Fig 6: Sensitivity analysis results

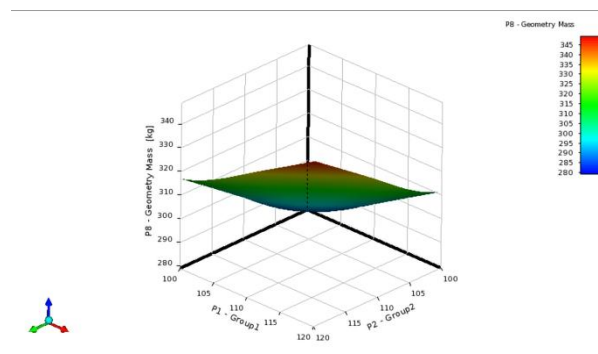
According to the sensitivity analysis, the selected 7 design variables have great influence on the weight, maximum deformation, maximum stress, seventh and eighth order natural frequencies of the frame, and the influence degree is also in line with the actual situation.

4.3 Response surface analysis

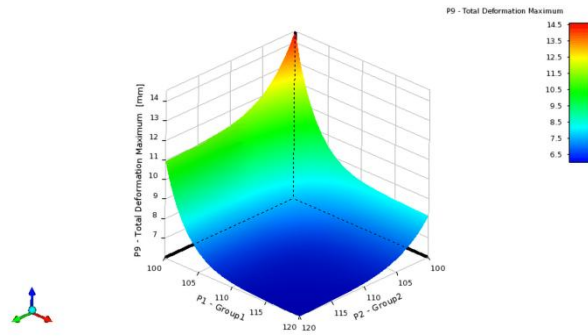
According to the test results, the second-order polynomial model is used as the response surface model for optimization analysis. The mathematical expression is as follows,

$$y(x) = \beta_0 + \sum_{i=1}^n \beta_i x_i^2 + \sum_{j=2}^n \sum_{i=1}^{j-1} \beta_{ij} x_i x_j \quad (3)$$

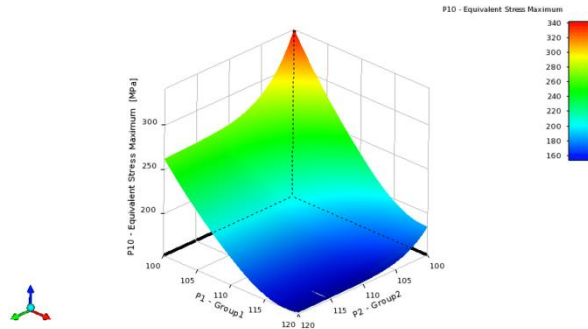
Where, $y(x)$ -- approximate value of response, x_i -- design variable, n -- number of variables, β -- Polynomial coefficients. The response surface between design variables and output parameters is constructed as shown in Figure 7.



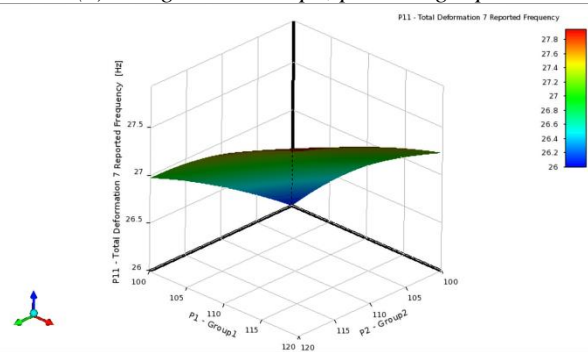
(a) Design variables p1, p2 -- weight p8



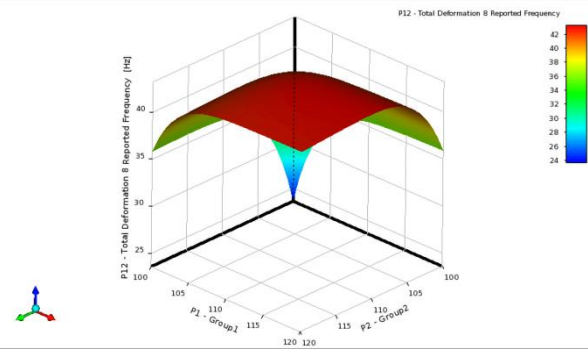
(b) Design variables p_1 , p_2 --maximum deformation p_9



(c) Design variables p_1 , p_2 -- weight p_{10}



(d) Design variables p_1 , p_2 --maximum deformation p_{11}



(e) Design variables p_1 , p_2 --maximum deformation p_{12}

Fig 7: Response surface

It can be concluded from Figure 7 that the design variables p_1 and p_2 have great influence on the weight, and p_1 , p_2 and p_5 have the greatest influence on the maximum deformation; p_1 , p_2 and p_7 have the greatest influence on the maximum stress and the seventh natural frequency; p_1 , p_2 and p_7 have the greatest influence on the eighth order natural frequency.

V. Lightweight Optimization of Frame

5.1 Optimization model

Combining the theory of frame optimization with practice, taking seven design variables as optimization design variables, combining constraints and design variables, the mathematical model is established as follows,

$$\begin{aligned} & \text{Find } x = (p_1, p_2, \dots, p_7)^T \\ & \text{Min } f(x_1) = p_8, p_9, p_{10} \\ & \text{Max } f(x_2) = p_{11}, p_{12} \\ & \text{S.t. } 1.4\sigma \leq 836 \\ & x^l \leq x \leq x^u \end{aligned}$$

Where $p_1 \sim p_7$ -- frame design variables, as shown in Table 5; $x^l = [100, 100, 36, 36, 36, 36, 36]^T$ -- lower limit of variables; $x^u = [120, 120, 44, 44, 44, 44, 44]^T$ -- upper limit of variables; $p_8 \sim p_{10}$ -- output parameters; 1.4 -- safety factor; 836 -- Material yield limit.

5.2 Lightweight optimization based on MOGA optimization algorithm

The mathematical model is optimized based on the MOGA optimization algorithm of Ansys-Workbench software optimization module. Under the constraints of variable, the optimization target is frame mass, maximum deformation, minimum maximum stress and the seventh and eighth order natural frequencies. After many times of optimization, the system gives three groups of candidate solutions satisfying variable constraints, as shown in Table 5.

Table 5 Candidate solution

	The first group	The second group	The third group
p_1/mm	106.08	105.55	104.81
p_2/mm	104.86	106.84	107.91
p_3/mm	36.129	36.841	39.071
p_4/mm	36.497	36.134	37.119
p_5/mm	36.209	37.561	36.257
p_6/mm	36.143	36.486	36.335
p_7/mm	36.458	36.69	36.292
p_8/kg	280.07	284.76	286.76
p_9/mm	7.43	7.44	7.71
p_{10}/MPa	189.5	179.8	180.4
p_{11}/HZ	23.786	24.37	24.522
p_{12}/HZ	39.094	39.83	39.846

5.3 Analysis of optimization results

The three groups of data in Table 5 are reasonable optimization solutions. According to the requirements of output parameters, the most reasonable optimization solution is selected. After analysis, the second group solution is selected as the optimization result, and the manufacturing process and other requirements are considered. The second group solution is rounded, and the optimization result is shown in Table 6.

Table 6 Optimization results

Design parameters	Before optimization/mm	After optimization/mm	After rounding/mm
p_1	110	105.55	106

p_2	110	106.84	107
p_3	40	36.841	37
p_4	40	36.134	36
p_5	40	37.561	38
p_6	40	36.486	36
p_7	40	36.69	37

Based on the rounded data in Table 6, the solid model of the frame is rebuilt in CATIA, and then imported into ANSYS for analysis and verification. The results are as follows: (1) After the lightweight optimization of the frame, the weight of the original frame is reduced from 314.42kg to 284.76kg, and the weight is reduced by 29.66kg, 9.43%. (2) After optimization, the stress of the frame is significantly reduced, and the maximum stress is reduced from 189.86MPa to 179.8MPa, with a reduction of 5.2%. The maximum stress after optimization meets the requirements. The maximum deformation increases from 6.54mm to 7.44mm. Although the maximum deformation increases, it still meets the stiffness requirements. (3) Under the condition of mass reduction, the frequency of the optimized frame is reduced, the seventh mode is reduced from 26.7HZ to 24.37 HZ, and the eighth mode is reduced from 42.08 HZ to 39.83 HZ. Although the frequency is reduced, it can stagger the road excitation and the vibration frequency of human organs when the vehicle is running normally, and the probability of resonance with the motor is small, which can meet the use requirements.

VI. Conclusion

Taking the TC4 titanium alloy light electric commercial vehicle frame as the research object, the static and dynamic characteristics of the frame are analyzed. Then, according to the load and size of the frame, the response surface model is established, and the size of the main load-bearing beam is optimized by using the MOGA optimization algorithm to realize the lightweight of the frame. The conclusions are as follows: (1) The weight of the frame is reduced from 314.42kg to 284.76kg, realizing the purpose of lightweight. After optimization, the maximum stress of the frame decreases from 189.86MPa to 179.8MPa, and the maximum deformation increases from 6.54mm to 7.44mm. Meet the design requirements of the frame. (2) The modal analysis shows that the low order frequency of the frame can stagger the road excitation and human organ vibration frequency, and the probability of resonance with the motor is small. Meet the frame design requirements. (3) From the fitting effect curve, it can be seen that the response surface model has high accuracy, and through sensitivity analysis, the results show that the size of the longitudinal beam is very sensitive to the maximum deformation, stress and weight of the frame, as well as the low-order mode, which further shows that the selected optimal size is reliable. The optimization design method can meet the multi-objective optimization design requirements of the frame.

Acknowledgments

This program was supported by the 2019 Research Program of Panzhihua University, China (Grant: 2019ZD002).

References

- [1] J.Q. Xu, Y.P. Yang, J. Tang, et al, "Comparative analysis on lightweight effect of pure electric vehicle and fuel vehicle," *Automotive Engineering*, vol. 34, no. 6, pp. 540-543, 2012.
- [2] J. Zhang, Y.L. Xie, "Research on lightweight optimization of a micro electric commercial vehicle frame," *Electromechanical Engineering*, vol. 37, no. 3, pp. 283-287, 2020.
- [3] Q.C.H. Wang, J.N. Zhao, F. Yang, et al, "Lightweight evaluation method and optimization design of truck frame," *Forging Technology*, vol. 42, no. 9, pp. 174-181, 2017.
- [4] J. Zhang, X.D. Long, "Lightweight optimization design and evaluation of electric bus frame," *Mechanical Design and Manufacturing*, no. 5, pp. 253-256, 2019.
- [5] K.C.H. Zhang, S.H.M. Li, M.J. Sun, "Lightweight optimization design of commercial vehicle frame with steel and aluminum materials under multiple working conditions," *China Mechanical Engineering*, vol. 31, no. 18, pp. 2206-2211 + 2219, 2020.

- [6] Y.W. Fu, L.P. Zhao, Y.B. Zhao, et al, "Application prospect of titanium alloy in oil and gas exploration and development," *Petroleum Drilling and Production Technology*, vol. 39, no. 5, pp. 662-666, 2017.
- [7] J. Zhang, W. Ran, "Lightweight Optimization Design of a Light Electric Commercial Vehicle Frame," *Journal of Physics: Conference Series*, vol. 1939, no.1, pp. 1-7, 2021.
- [8] C.H.L. Yang, Y.L. Zhang, W. Huang, et al, "Structural analysis and optimization design of new electric vehicle frame," *Mechanical Design and Manufacturing*, no. 6, pp. 234-237, 2017.
- [9] D.S.H. Lu, D.F. Wang, X.P. Su, "Finite element analysis of a bus frame based on HyperWorks," *Mechanical Design and Manufacturing*, no. 3, pp. 11-12, 2011.
- [10] J. Zhang, K.R. Chen, B. Zheng, "Lightweight optimization design of new electric vehicle frame," *Manufacturing Automation*, vol. 41, no. 3, pp. 51-55, 2019
- [11] Z.N. Zhang, ZH.J. Xi, Y.P. Liu, et al, "Structural strength and modal analysis of the frame of a vehicle mounted pressure fixing equipment," *Petroleum Machinery*, vol. 47, no. 3, pp. 68-74 + 80, 2019.
- [12] J. Zhang, K.R. Chen, Y.P. Dai, "Design and modal analysis of electric vehicle frame for modern agricultural manor," *China Agricultural Machinery Chemical Journal*, vol. 40 no. 2, pp. 109-112, 2019.
- [13] F.Y. Cao, J.J. Li, M.K. Cui, et al, "Multidisciplinary optimization of frame structure of small and medium truck crane," *Mechanical Design and Manufacturing*, no. 3, pp. 39-42, 2020.